Eur. Phys. J. A **27**, 91–97 (2006)
DOI 10.1140/epja/i2005-10212-2

THE EUROPEAN PHYSICAL JOURNAL A

Measurement of the LT-asymmetry in π^0 electroproduction at the energy of the $\Delta(1232)$-resonance

D. Elsner[1,a], A. Süle[1,b], P. Barneo[2], P. Bartsch[3], D. Baumann[3], J. Bermuth[3], R. Böhm[3], D. Bosnar[3,c], M. Ding[3], M. Distler[3], D. Drechsel[3], I. Ewald[3], J. Friedrich[3], J.M. Friedrich[3,d], S. Grözinger[3,e], P. Jennewein[3], S. Kamalov[3], F. H. Klein[1], M. Kohl[4,f], K.W. Krygier[3], H. Merkel[3], P. Merle[3], U. Müller[3], R. Neuhausen[3], Th. Pospischil[3], M. Potokar[5], G. Rosner[3,g], H. Schmieden[1], M. Seimetz[3,h], O. Strähle[3], L. Tiator[3], Th. Walcher[3], and M. Weis[3]

[1] Physikalisches Institut, Rheinische Friedrich-Wilhelms-Universität, D-53115 Bonn, Germany
[2] NIKHEF, Amsterdam, The Netherlands
[3] Institut für Kernphysik, Johannes Gutenberg-Universität, D-55099 Mainz, Germany
[4] Institut für Kernphysik, Technische Universität Darmstadt, D-64289 Darmstadt, Germany
[5] Institut Jožef Stefan, University of Ljubljana, SI-1001 Ljubljana, Slovenia

Received: 15 July 2005 / Revised version: 15 December 2005 /
Published online: 6 February 2006 –
Communicated by M. Garçon

Abstract. The reaction $p(e,e'p)\pi^0$ has been studied at $Q^2 = 0.2$ (GeV/c)^2 in the region of $W = 1232$ MeV. From measurements left and right of $\mathbf{q}$, cross-section asymmetries ρ_{LT} have been obtained in forward kinematics $\rho_{LT}(\theta^{cm}_{\pi^0} = 20^\circ) = (-11.68 \pm 2.36_{stat} \pm 2.36_{sys})$ and backward kinematics $\rho_{LT}(\theta^{cm}_{\pi^0} = 160^\circ) = (12.18 \pm 0.27_{stat} \pm 0.82_{sys})$ π^0. Multipole ratios $\Re\{S^*_{1+}M_{1+}\}/|M_{1+}|^2$ and $\Re\{S^*_{0+}M_{1+}\}/|M_{1+}|^2$ were determined in the framework of the MAID2003 model. The results are in agreement with older data. The unusally strong negative $\Re\{S^*_{0+}M_{1+}\}/|M_{1+}|^2$ required to bring also the result of Kalleicher *et al.* in accordance with the rest of the data is almost excluded.

PACS. 13.60.Le Meson production – 13.40.-f Electromagnetic processes and properties – 14.20.Gk Baryon resonances with $S = 0$

1 Introduction

The nucleon ground- and excited-state properties presently elude a consistent description in terms of QCD as the basic theory of strong interaction, due to the non-linear, non-perturbative interaction of quarks and gluons. Over the last years, considerable efforts aimed at a better understanding of this complicated structure, both theoretically and experimentally. One important issue is the understanding of the "shape" of the nucleon. Despite its spin of 1/2 and, in consequence, the vanishing spectroscopic quadrupole moment, the nucleon wave function might have quadrupole components which are expected to exhibit in the transition of the ground state to the spin-(3/2) $\Delta(1232)$ excitation. Within constituent quark models those components originate from tensor forces generated by a color hyperfine interaction [1–4]. Larger quadrupole strengths are expected from models emphasizing the particular role of pions via exchange currents [5] or the "pion cloud" [6–10], and also in first quenched Lattice QCD calculations [11]. Dynamical approaches [12–14] enable a decomposition into the "bare" contributions, as described in quark models, and the "dressing" by the pion cloud.

The quadrupole strength is usually characterized by the ratios $R_{\rm EM} = E_{1+}/M_{1+}$ and $R_{\rm SM} = S_{1+}/M_{1+}$ of the πN multipoles in the $\Delta(1232) \to N\pi$ decay[1], which are uniquely related to the photon multipoles of electromagnetic excitation [17,18]. Hence, these ratios can be measured in photo- and electroproduction of pions in the energy region of the $\Delta(1232)$-resonance. Since unwanted

[a] e-mail: elsner@physik.uni-bonn.de (corresponding author)
[b] e-mail: suele@physik.uni-bonn.de
[c] *Permanent address*: Department of Physics, University of Zagreb, Croatia.
[d] *Present address*: Physik Department E18, TU München, Germany.
[e] *Present address*: GSI, Darmstadt, Germany.
[f] *Present address*: MIT/Bates, Massachusetts, USA.
[g] *Present address*: Department of Physics and Astronomy, University of Glasgow, UK.
[h] *Present address*: DAPNIA/SPhN, CEA Saclay, France.

[1] For the exact definition and aspects of isospin separation, see [15,16].

non-resonant contributions are strongly suppressed in the π^0 channel compared to the charged pion production, most measurements focused on the $\gamma^{(*)}p \to p\pi^0$ reaction.

A number of studies pursued at the laboratories providing cw electron beams yielded precise coincidence data based on high-luminosity beams and high-resolution detectors with large angular coverage. Partially single- or double-polarization observables have been measured. The evolution of $R_{\rm EM}$ and $R_{\rm SM}$ with negative squared four-momentum transfer, Q^2, has been investigated over a large range in Q^2 up to $4\,(\mathrm{GeV}/c)^2$ [19–21]. The extraction of the quadrupole ratios from the measured cross-sections is non-trivial. For the $R_{\rm SM}$ discussed here, it is more reliable at lower Q^2, where the M_{1+} dominance is more pronounced than at higher Q^2 and single- [22,23] and double-polarization results [24–26] are already available in addition to unpolarized recent measurements [20,21,27–30]. The low-Q^2 results are almost all compatible with each other, yielding $R_{\rm SM} \simeq -6\%$, cf. fig. 5. The only exception is the result of Kalleicher *et al.* [27]. However, due to the particular kinematics it could be interpreted in line with the other results, if the ratio $S_{0+}/M_{1+} \simeq -10\%$ [16]. S_{0+} is related to the spin $1/2 \to 1/2$ transition. This amplitude was neglected in the analysis of [27]. Both magnitude and sign of such an S_{0+} are however unexpected from models, *e.g.* MAID2003 [18], but not excluded by older measurements with large errors [31,32] which yielded slightly positive values with errors of the order 10% absolute.

In order to investigate this issue, measurements of π^0 electroproduction in forward and backward direction have been performed, which are reported in this paper. It is organized as follows: in the next section the cross-section formalism is briefly summarized and the method is motivated. The description of the experiment is then followed by a discussion of the data analysis, systematic-error contributions and the results in sects. 5, 6 and 7.

2 Cross-section of pion electroproduction

In one-photon-exchange approximation the fivefold differential cross-section of pion electroproduction

$$\frac{\mathrm{d}^5\sigma}{\mathrm{d}E_e \mathrm{d}\Omega_e \mathrm{d}\Omega_\pi^{cm}} = \Gamma \frac{\mathrm{d}^2\sigma_v}{\mathrm{d}\Omega_\pi^{cm}} \tag{1}$$

factorizes into the virtual photon flux

$$\Gamma = \frac{\alpha}{2\pi^2}\frac{E'}{E}\frac{k_\gamma}{Q^2}\frac{1}{1-\epsilon} \tag{2}$$

and the virtual photon cm cross-section $\mathrm{d}^2\sigma_v/\mathrm{d}\Omega_\pi^{cm}$. Here α denotes the fine-structure constant, $k_\gamma = (W^2 - m_p^2)/2m_p$ the laboratory energy of a real photon for the excitation of the target with mass m_p to the cm energy W, and $\epsilon = [1+(2|\mathbf{q}|^2/Q^2)\tan^2\frac{\vartheta_e}{2}]^{-1}$ the photon polarization parameter. $Q^2 = |\mathbf{q}|^2 - \omega^2$ is the negative squared four-momentum transfer, $\mathbf{q}$ and ω are the three-momentum and energy transfers, respectively, and E, E' and ϑ_e the incoming and outgoing electron energy and the electron scattering angle in the laboratory frame.

The unpolarized cross-section for pion production with virtual photons is given by [17,18]

$$\frac{\mathrm{d}^2\sigma_v}{\mathrm{d}\Omega_\pi^{cm}} =: \sigma_v = \sigma_T + \epsilon_L\sigma_L + \sqrt{2\epsilon_L(1+\epsilon)}\sigma_{LT}\cos\phi + \epsilon\sigma_{TT}\cos 2\phi. \tag{3}$$

The partial differential cross-sections, for which we use the short-hand notation σ_i, describe the response of the hadronic system to the polarization of the photon field, characterized by the degrees of transverse (T) and longitudinal (L) polarization, ϵ and $\epsilon_L = \frac{Q^2}{\omega_{cm}^2}\epsilon$, respectively. The angle ϕ is the tilting angle between the electron scattering plane and the reaction plane. At $\phi = 0°$ and $180°$ ($\phi = 90°$ and $270°$) pions are ejected in (perpendicularly to) the scattering plane.

3 Method

The partial cross-section σ_{LT} is sensitive to both S_{0+} and S_{1+}. It can be determined from a fit of the ϕ-dependence of the cross-section of eq. (3). To this end, two measurements left ($\phi = 0°$) and right ($\phi = 180°$) of the $\mathbf{q}$-direction are sufficient, which allow to form the asymmetry

$$\rho_{LT}(\theta_{\pi^0}^{cm}) := \frac{\sigma_v(\phi = 0°) - \sigma_v(\phi = 180°)}{\sigma_v(\phi = 0°) + \sigma_v(\phi = 180°)} \tag{4}$$

as a function of the π^0 center-of-mass polar angle, $\theta_{\pi^0}^{cm}$. According to eq. (3), it is related to the partial cross-sections via

$$\rho_{LT}(\theta_{\pi^0}^{cm}) = \frac{\sqrt{2\epsilon_L(\epsilon+1)}\sigma_{LT}}{\sigma_T + \epsilon_L\sigma_L + \epsilon\sigma_{TT}}. \tag{5}$$

The sensitivity to S_{0+} and S_{1+} is shown by a partial-wave decomposition of eq. (5), where only the leading multipoles are retained. At the $\Delta(1232)$-resonance position the asymmetry

$$\rho_{LT}(\theta_{\pi^0}^{cm}) \simeq f(\theta_{\pi^0}^{cm}) \cdot \frac{\Re\{(S_{0+}^* + 6S_{1+}^*\cos\theta_{\pi^0}^{cm})M_{1+}\}}{|M_{1+}|^2} \tag{6}$$

is obtained. Thus measurements of ρ_{LT} in the forward (θ_1) and backward cm-hemisphere ($\theta_2 = \pi - \theta_1$) allow the extraction of S_{1+}/M_{1+} and S_{0+}/M_{1+}:

$$\frac{\Re\{S_{1+}^* M_{1+}\}}{|M_{1+}|^2} = f_1(\theta_{1,2}) \cdot [\rho_{LT}(\theta_1) - \rho_{LT}(\theta_2)] + C_1, \tag{7}$$

$$\frac{\Re\{S_{0+}^* M_{1+}\}}{|M_{1+}|^2} = f_0(\theta_{1,2}) \cdot [\rho_{LT}(\theta_1) + \rho_{LT}(\theta_2)] + C_0. \tag{8}$$

The functions $f_0(\theta_{1,2})$ and $f_1(\theta_{1,2})$ denote kinematical factors, C_0 and C_1 contain contributions of multipoles beyond the approximation.

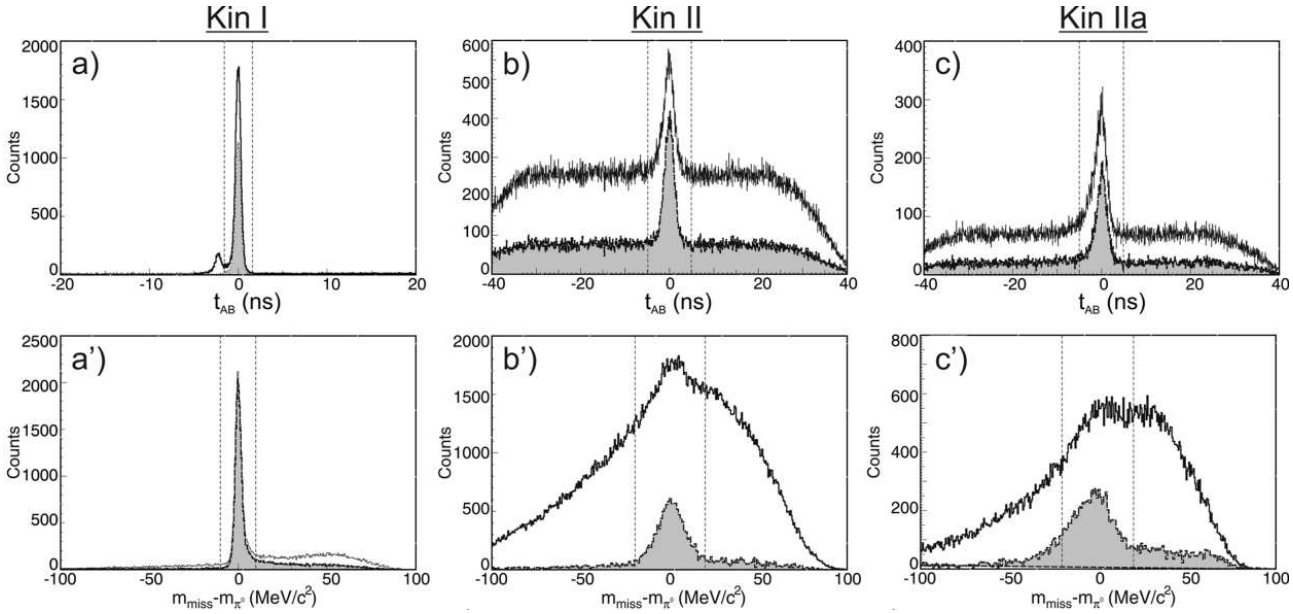

Fig. 1. Typical coincidence time (a,b,c) and missing-mass (a′,b′,c′) spectra for Kin. I, II and IIa. Light spectra result from standard cuts without phase-space restrictions. Shaded time spectra (FWHM peaks: (a) 0.8 ns, (b) 2.7 ns, (c) 3.0 ns) result from missing-mass cuts (dashed vertical lines in the missing-mass plots) around the π^0 mass; in Kin. I and Ia (not shown) the cut eleminates the π^- time peak and at Kin. II and IIa the prompt time peak becomes symmetric (see text). The shaded missing-mass spectra result similarly from the indicated cuts around the coincidence time peak.

4 Experiment

The $p(e,e'p)\pi^0$ experiment was performed at the Mainz Microtron MAMI [33] using a beam energy of 855 MeV and currents of $\sim$ 33 μA which were measured with high precision by a Förster probe in the recirculation path of the 3rd microtron stage. The beam hit a liquid-hydrogen target. Specifically designed for this experiment, the $\varnothing$1 cm cylindrical target cell with 6.25 μm Havar walls [34] enabled the detection of very low-energetic protons. The scattered electrons were detected at a central angle $\theta_{e^-}^{lab} = 44.45°$ and central momentum $p = 408.7$ MeV/c in the Spectrometer A of the Three-Spectrometer setup of the A1 Collaboration [35]. It consists of a QSDD magnetic system and is equipped with two double planes of vertical drift chambers for measurement of particle trajectories in the focal plane. During the course of the measurements presented here, the standard Cherenkov detector for π^-/e^--discrimination was not available, since it was replaced by a focal-plane proton polarimeter [36] for other experiments [24,37]. In coincidence with the scattered electron, the recoil protons of the $p(e,e'p)\pi^0$ reaction were detected in the Spectrometer B with a similar focal-plane instrumentation. The smallest possible angle between the Spectrometer B and the exit beam-pipe is 9° and the momentum threshold for the proton detection is 250 MeV/c. Hence $Q^2 = 0.2$ (GeV/c)^2 was the minimum possible momentum transfer that could be reached at $W = 1232$ MeV. The four different kinematic settings are summarized in table 1. In order to check for false asymmetries, possibly caused by inefficiencies of the focal-plane detectors in the proton arm, the Spectrometer B was displaced by 1° against the nominal setting for part of the measurements. The π^0 data were supplemented by elastic $p(e,e'p)$ measurements (table 2) to monitor the overall experimental consistency with high precision. The overdetermined kinematics allows comparison of every measured variable with the values calculated from the other measured variables. Corrections of 0.5 MeV/c for the central momentum of the electron spectrometer and 0.1° for the angle of the proton spectrometer were determined. The probable origin is a very slight mismatch between hardware (detector angle, field integral) and the track reconstruction.

Precise measurements of electron beam current and dead time allowed an accurate determination of the effective luminosity.

Table 1. Proton kinematics.

Kin.	$\theta_{\pi^0}^{cm}$ (°)	ϕ (°)	p_p^{lab} (MeV/c)	θ_p^{lab} (°)
I	160	0	741.7	33.0/32.0
Ia		180		20.9/21.9
II	20	0	265.02	44.2/43.7
IIa		180		9.8/10.3

Table 2. Elastic scattering kinematics.

Spec. A (electron)		Spec. B (proton)		Beam
θ (°)	p (MeV/c)	θ (°)	p (MeV/c)	E (MeV)
55.5	612.0	43.6–46.0	704.4	855.0
46.5	314.6	58.4, 59.4	251.0	351.3

5 Data analysis

Typical coincidence time and missing-mass spectra are shown in fig. 1. The overdetermined kinematics allows the reconstruction of the unobserved π^0 by its missing mass, $m^{\pi^0}_{miss}$. Basic background reduction is obtained by coincidence time cuts and subtraction of random coincidences via sidebands. In addition to the almost background-free e'-p coincidence peak, the time spectrum for the high proton momentum kinematics shows a smaller second peak at ~ -2.2 ns (Kin. I, cf. fig. 1a). It is caused by negative pions, predominantly from $\pi^+\pi^-$ reactions, the π^- of which are detected in the electron spectrometer after a longer flight time compared to electrons. These events can be eliminated by the coincidence time cut indicated in fig. 1a. However, for Kin. II and IIa, the unwanted negative pions can no longer be separated by coicidence time, due to insufficient time resolution caused by multiple scattering at the low proton momentum. Instead, additional missing-mass cuts are used to suppress these events. As also illustrated in fig. 1, with a cut around m_{π^0} (a′, b′, c′) the π^- peak vanishes in Kin. I (shaded area of fig. 1a). Under the conditions of Kin. II/IIa the resulting coincident-time peak becomes symmetric after the missing-mass cut.

Standard cuts ensure valid track reconstruction in both spectrometers. No target-vertex cuts were applied in order to avoid artificial ρ_{LT}-asymmetries from the very different vertex resolution along the beam direction for the different settings. Spectrometer acceptances were normalised with standard Monte Carlo phase-space simulations, which also include the radiative corrections [38].

The limited spectrometer acceptances cause different correlations between $W, Q^2, \epsilon, \theta^{cm}_{\pi^0}$ and ϕ for the settings left and right of $\mathbf{q}$, as illustrated in fig. 2. Due to these correlations, equal binning in the variables nevertheless leads to unequal distributions left and right of $\mathbf{q}$. Thus artificial ρ_{LT}-asymmetries can be generated, if the mean values of the kinematic variables differ between left (l) and right (r). This is obvious, *e.g.*, for a case where $W_l = 1232\,\mathrm{MeV} - \delta$ and $W_r = 1232\,\mathrm{MeV} + \delta$, since the trivial W-dependence of the cross-section produces a $\rho_{LT} \neq 0$.

It is extremely important to base the experimental asymmetries on left-right bins with the same mean values of the variables $W, Q^2, \theta^{cm}_{\pi^0}$ and ϕ. This is ensured by projection of the numbers measured in each bin to the same "nominal kinematics". For this projection we made use of the MAID2000 parametrisation. The projection factors are obtained as the calculated ratios of differential cross-sections. In order to minimise the projection error, only data are used within the $\theta^{cm}_{\pi^0}$-W overlap region of the two acceptance bands in fig. 2. Remaining uncertainties are included in the systematic error.

The appropriately normalised and projected numbers of events left and right of $\mathbf{q}$ are determined by

$$n_{l(\phi=0^\circ),r(\phi=180^\circ)} = \frac{\sum_{Bins}(N_{l,r}/P_{l,r}) \cdot \mathrm{MAID}^{corr}_{l,r}}{L_{l,r}}. \quad (9)$$

Here $N_{l,r}$ denotes the number of counts after cuts, which has to be divided by the relative phase-space acceptance

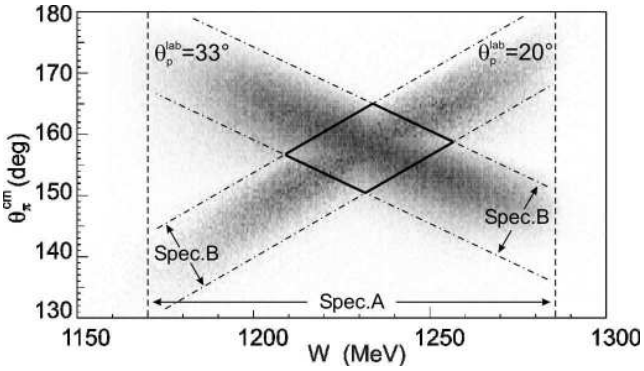

Fig. 2. Spectrometer acceptances for left ($\theta^{lab}_p = 33^\circ$) and right ($\theta^{lab}_p = 20^\circ$) settings of kinematics I. W is limited by the electron spectrometer (A) acceptance. The angular acceptance of the proton spectrometer (B) determines the width in $\theta^{cm}_{\pi^0}$.

$P_{l,r}$. $\mathrm{MAID}^{corr}_{l,r}$ is the projection factor and $L_{l,r}$ represents the relative luminosity. The asymmetry is then simply given by

$$\rho_{LT}(\theta^{cm}_{\pi^0}) = \frac{n_l - n_r}{n_l + n_r}. \quad (10)$$

6 Systematic errors

The systematic error has been estimated for Kin. I/Ia from the data themselves by variation of all kinematic cuts. For the data with low proton momentum (Kin. II/IIa) such an analysis is limited by the available statistics and experimental resolution. The sliding cuts in the variables W and $m^{\pi^0}_{miss}$ resulted in non-negligible systematic errors (table 3a, 3b). The sliding cut in $m^{\pi^0}_{miss}$ sets a limit on remaining radiative effects beyond those included in the phase-space simulation. The spectrometer correction, which was determined by elastic measurements, has been taken into account both in analysis (track reconstruction) and simulation. The value given in table 3c results from the variation of the angle of the Spectrometer B by $\pm 0.1^\circ$. Potential error contributions of the MAID projection were estimated through the relative variation of M_{1+} by $\pm 5\%$ and, simultaneously, of S_{1+} and S_{0+} by $\pm 50\%$ in the full MAID2000 calculation. The largest deviation is given in table 3d. Additional errors for the luminosity determination are not required. The maximum variations of 2% relative were corrected, and the remaining effect is negligible. All kinematic settings were measured repeatedly to avoid time-dependent effects, *e.g.* efficiency variations. These data sub-sets were combined for the left and right kinematics.

Table 3. Absolute systematic errors ($\Delta\rho_{LT}$) of high proton momentum kinematics.

a) W cut	0.29%
b) $m^{\pi^0}_{miss}$ cut	0.23%
c) Spectrometer corrections	0.57%
d) MAID2000 projection	0.46%

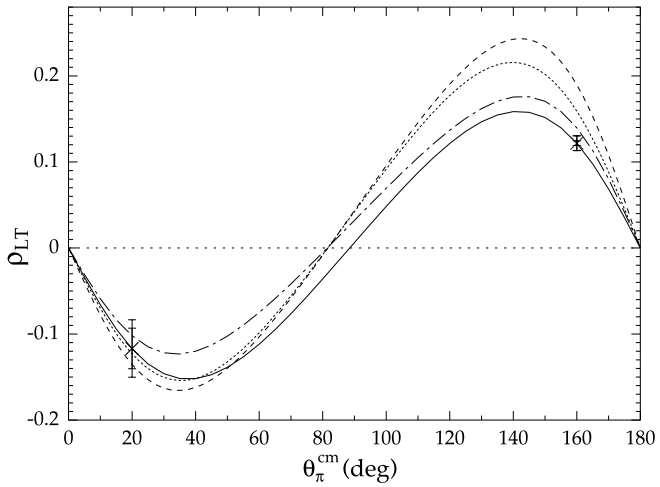

Fig. 3. The measured ρ_{LT}-asymmetries compared with model predictions from MAID2003 [18] (dotted line), DMT2001 [12, 13] (dashed line), Sato/Lee [14] (dash-dotted line). The full curve represents the MAID2003 re-fit reported in this paper. The depicted errors represent the statistical (inner bars) and the quadratic sum of the statistical and systematical errors (outer bars) as discussed in the text.

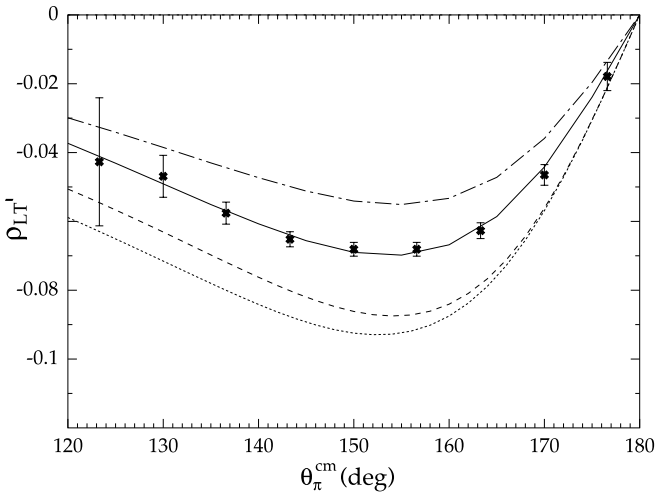

Fig. 4. Results for $\rho_{LT'}$ from ref. [23] with model predictions from MAID2003 [18] (dotted line), DMT2001 [12,13] (dashed line), Sato/Lee [14] (dash-dotted line). The full curve represents the MAID2003 re-fit. The depicted errors are only statistical.

7 Results and discussion

From eq. (10) the asymmetries

$$\rho_{LT}(\theta_{\pi^0}^{cm} = 160^\circ) = (12.18 \pm 0.27_{stat} \pm 0.82_{sys})\%,$$
$$\rho_{LT}(\theta_{\pi^0}^{cm} = 20^\circ) = (-11.68 \pm 2.36_{stat} \pm 2.36_{sys})\%$$

are determined. The total systematic error is obtained by quadratic summation of the individual contributions in table 3. For the forward measurement a systematic error of the same size as its statistical one is assumed as the worst case estimate. Using these new data in conjunction with the previous measurement of the $\rho_{LT'}$-asymmetry (fifth structure function) of Bartsch *et al.* [23], we performed a re-fit of the MAID2003 parameters. We obtained sensitivity to real and imaginary parts of the S_{1+} and S_{0+} amplitudes in the $p\pi^0$ channel. The results for ρ_{LT} and $\rho_{LT'}$ are depicted in figs. 3 and 4 which, for comparison, also show the standard MAID2003 and the calculation within the dynamical models of Kamalov/Yang (DMT2001) [12, 13] and Sato/ Lee [14].

From our MAID re-fit we extract the results given in the first row in table 4. The denoted errors are due to the re-fit of S_{1+} and S_{0+} within the MAID2003 analysis taking into account the statistical and systematical errors. The model dependence of the extraction can be estimated from the truncated multipole result given in the second row in table 4. In the framework of this approximation we extract from the measured ρ_{LT}-asymmetries the multipole ratios via eqs. (7) and (8) with only leading terms in S_{1+}, S_{0+} and M_{1+}. The last two lines in table 4 contain standard model values without re-fit to our data.

Table 4. Comparison of multipole ratios from data and calculations, as discussed in the text.

	$\frac{\Re\{S_{1+}^* M_{1+}\}}{\lvert M_{1+}\rvert^2}$ (%)	$\frac{\Re\{S_{0+}^* M_{1+}\}}{\lvert M_{1+}\rvert^2}$ (%)
MAID2003 re-fit	-5.45 ± 0.42	2.56 ± 2.25
From eqs. (7), (8)	-4.78 ± 0.69	0.56 ± 3.89
MAID2003	-6.65	7.98
Sato/Lee	-4.74	5.14

Figure 5 shows our full MAID2003 result for $R_{\rm SM}$. Within the errors, our extracted value is in accordance with measurements at the same Q^2 [28] and measurements at adjacent Q^2 [21,24]. The negative-slope tendency of the CLAS data [21] seems to be further supported by our $R_{\rm SM}$ value at smaller Q^2. Provided there is no sharp Q^2-dependence in $R_{\rm SM}$, we can rule out the result of Kalleicher *et al.* [27] at $Q^2 = 0.127$ (GeV/c)^2. This has been argued before from measurements in backward kinematics [29] where an S_{0+} contribution cannot be excluded. In contrast, our conclusion comes from forward kinematics as also exploited by [27]. This is illustrated in fig. 6. It shows on a different scale the same ρ_{LT}-asymmetry as fig. 3, the MAID2003 re-fit and a full MAID2003 calculation using the multipole ratios S_{0+}/M_{1+} and S_{1+}/M_{1+} of Kalleicher *et al.* In addition, a full MAID2003 calculation using $S_{0+}/M_{1+} \simeq -10\%$, which could reconcile the Kalleicher result with others [16], is shown. However, this is clearly excluded by our measurement at $\theta_{\pi^0}^{cm} = 20^\circ$ with a 4σ significance.

Our S_{0+}/M_{1+} ratio, extracted from the MAID2003 re-fit, is plotted in fig. 7. Within the errors it agrees with older data at slightly larger Q^2 [31,32]. Although a little lower, it is also compatible with the Sato/Lee, DMT2001 and standard MAID2003 parametrisations. In view of the quite large experimental errors it is not yet clear whether

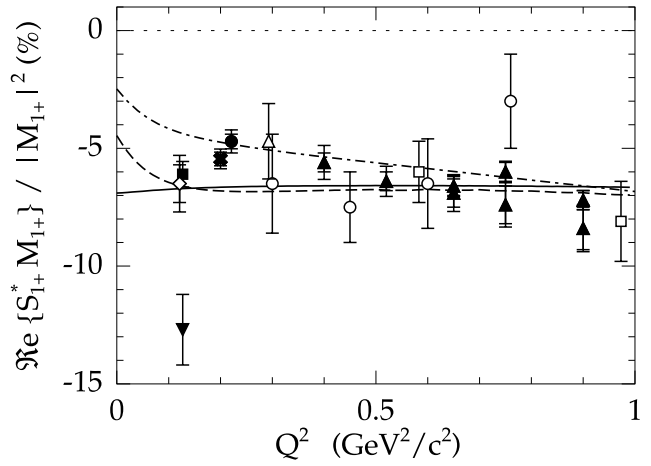

Fig. 5. Result for $\Re\{S_{1+}^{*}M_{1+}\}/|M_{1+}|^2$ with statistical and systematical errors as extracted from this experiment using the MAID2003 re-fit (full cross), compared to measurements. Data where only statistical errors are given: DESY [31] (open squares), NINA [32] (open circles), Bonn synchrotron [39] (open triangle tip up) and ELSA [27] (full triangle tip down). Data, where statistical and systematical errors are given: ELSA [28] (full circle, shifted from $Q^2 = 0.201$ (GeV/c)^2 to $Q^2 = 0.221$ (GeV/c)^2 for clarity), MAMI [24] (open diamond), CLAS [21] (full triangles) and BATES [29,30] (full square). The curves show model calculations MAID2003 [18] (solid), DMT2001 [13] (dashed) and Sato/Lee [14] (dash-dotted).

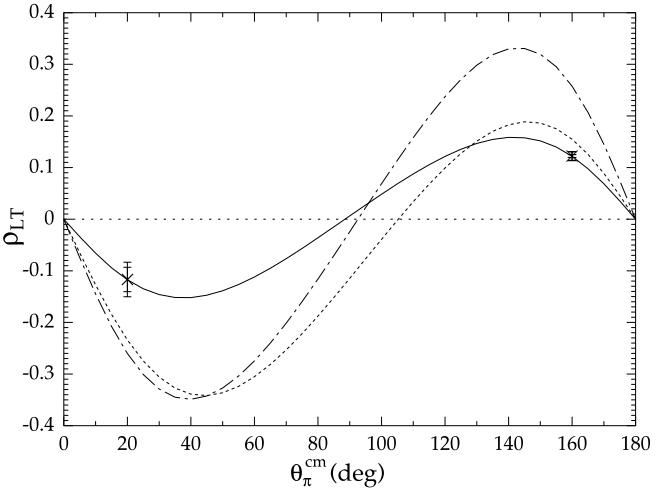

Fig. 6. The plot shows, at smaller scale, the MAID2003 re-fit (solid line) in comparison to the full MAID2003 calculation with modified $\Im\{S_{1+}\}$ and $\Im\{S_{0+}\}$ for two situations: $S_{1+}/M_{1+} = -12.5\%$, $S_{0+}/M_{1+} = 0.0\%$ (dash-dotted line), *i.e.* the result of [27], and $S_{1+}/M_{1+} = -10\%$, $S_{0+}/M_{1+} = -14\%$ (dotted line), which would bring [27] in accordance with other measurements [16].

this ratio differs from zero. But we cannot support a large negative S_{0+}/M_{1+} ratio.

A sensitive access to the ratio S_{0+}/S_{1+} is provided by a precise measurement of the zero crossing of ρ_{LT} or σ_{LT}. By now it is possible to extract this ratio from available data close to the zero crossing at $Q^2 = 0.127$ (GeV/c)^2 [30], with the result compatible to the MAID2003 parametrisation. Other existing data [21] cover the full range of $\theta_{\pi^0}^{cm}$ at $Q^2 = 0.4$–1.8 (GeV/c)^2. However, at higher Q^2 the S_{0+} extraction seems to be affected more strongly by higher partial waves than expected in the paper by Joo *et al.* [21]. This might be resolved by very recent polarisation data [40,41].

In future experiments at MAMI-C a more accurate determination of S_{0+} at low Q^2 is feasible, using the Three-Spectrometer setup of the A1 Collaboration complemented by the KaoS spectrometer [42].

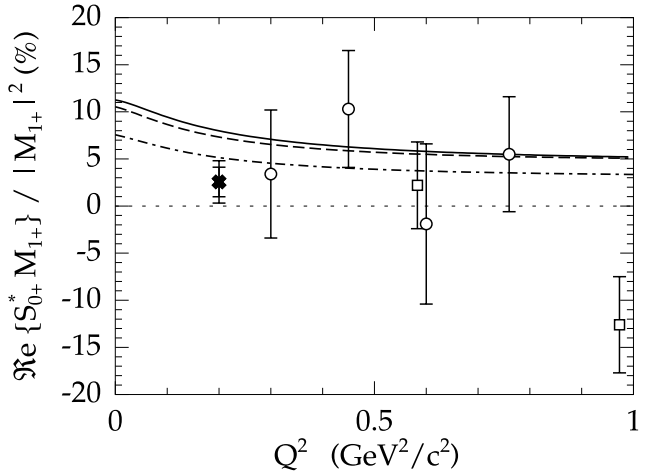

Fig. 7. Result for $\Re\{S_{0+}^{*}M_{1+}\}/|M_{1+}|^2$ with statistical and systematical errors as extracted from this experiment using the MAID2003 re-fit (full cross); compared to measurements from DESY [31] (open squares), NINA [32] (open circles), where only statistical errors are indicated. The curves show model calculations MAID2003 [18] (solid), DMT2001 [13] (dashed) and Sato/Lee [14] (dash-dotted).

8 Summary

We have measured the ρ_{LT}-asymmetry in forward ($\theta_{\pi^0}^{cm} = 20°$) and backward ($\theta_{\pi^0}^{cm} = 160°$) kinematics of π^0 electroproduction off the proton at $Q^2 = 0.2$ (GeV/c)^2 around $W = 1232$ MeV. The measurement of the two kinematic settings allows the extraction of S_{1+} and S_{0+} in a very transparent way within a simple s- and p-wave approximation or, alternatively, using the full MAID2003 parametrisation without any truncation. Our results for S_{1+}/M_{1+} and S_{0+}/M_{1+} are in agreement with existing measurements and calculations. Our result removes a remaining possibility to reconcile the datum of Kalleicher *et al.* [27] for the ratio S_{1+}/M_{1+} with other measurements through a large negative S_{0+}/M_{1+}.

We thank T.-S.H. Lee and T. Sato for providing their calculations. This work was supported by the Deutsche Forschungsgemeinschaft (SFB 443).

References

1. A. de Rújula, H. Georgi, S.L. Glashow, Phys. Rev. D **12**, 147 (1975).
2. N. Isgur, G. Karl, R. Koniuk, Phys. Rev. D **25**, 2394 (1982).
3. S.S. Gershtein, G.V. Dzhikiya, Sov. J. Nucl. Phys. **34**, 870 (1982).
4. D. Drechsel, M.M. Giannini, Phys. Lett. B **143**, 329 (1984).
5. A.J. Buchmann *et al.*, Phys. Rev. C **58**, 2478 (1998).
6. K. Bermuth *et al.*, Phys. Rev. D **37**, 89 (1988).
7. H. Walliser, G. Holzwarth, Z. Phys. A **357**, 317 (1997).
8. G.C. Gellas *et al.*, Phys. Rev. D **60**, 054022 (1999).
9. A. Silva *et al.*, Nucl. Phys. A **675**, 637 (2000).
10. L. Amoreira, P. Alberto, M. Fiolhais, Phys. Rev. C **62**, 045202 (2000).
11. C. Alexandrou, Phys. Rev. Lett. **94**, 021601 (2005).
12. S.S. Kamalov, S.N. Yang, Phys. Rev. Lett. **83**, 4494 (1999).
13. S.S. Kamalov, S.N. Yang, D. Drechsel, L. Tiator, Phys. Rev. C **64**, 032201 (2001).
14. T. Sato, T.-S.H. Lee, Phys. Rev. C **63**, 055201 (2001).
15. H. Schmieden Eur. Phys. J. A **1**, 427 (1998).
16. H. Schmieden, *Proceedings of NSTAR2001*, edited by D. Drechsel, L. Tiator, (World Scientific, 2001) p. 27.
17. D. Drechsel, L. Tiator, J. Phys. G **18**, 449 (1992).
18. D. Drechsel, O. Hanstein, S.S. Kamalov, L. Tiator, Nucl. Phys. A **645**, 145 (1999), `http://www.kph.uni-mainz.de/MAID/maid2000/`.
19. V.V. Frolov *et al.*, Phys. Rev. Lett. **82**, 45 (1999).
20. R.W. Gothe, Prog. Part. Nucl. Phys. **44**, 185 (2000).
21. K. Joo *et al.*, Phys. Rev. Lett. **88**, 122001 (2002).
22. G. Warren *et al.*, Phys. Rev. C **58**, 1998) 3722
23. P. Bartsch *et al.*, Phys. Rev. Lett. **88**, 142001 (2002).
24. Th. Pospischil *et al.*, Phys. Rev. Lett. **86**, 2959 (2001).
25. L.D. van Buuren *et al.*, Phys. Rev. Lett. **89**, 012001 (2002)
26. A. Biselli *et al.*, Phys. Rev. C **68**, 35202 (2003).
27. F. Kalleicher *et al.*, Z. Phys. A **359**, 201 (1997).
28. D. Wacker, PhD Thesis, Institut für Strahlen- und Kernphysik, University Bonn (1998).
29. C. Mertz *et al.*, Phys. Rev. Lett. **86**, 2963 (2001).
30. N.F. Sparveris *et al.*, Phys. Rev. Lett. **94**, 022003 (2005).
31. R. Siddle *et al.*, Nucl. Phys. B **35**, 93 (1971).
32. J.C. Alder *et al.*, Nucl. Phys. B **46**, 573 (1972).
33. H. Herminghaus, in *Proceedings of the 1990 Linear Accelerator Conference, Albuquerque, NM, 1990*, unpublished; T. Walcher, Prog. Part. Nucl. Phys. **24**, 189 (1990).
34. D. Elsner, diploma thesis, Institut für Kernphysik, University Mainz (2000).
35. K.I. Blomqvist *et al.*, Nucl. Instrum. Methods A **403**, 263 (1998).
36. Th. Pospischil *et al.*, Nucl. Instrum. Methods A **483**, 713 (2002).
37. Th. Pospischil *et al.*, Eur. Phys. J. A **12**, 125 (2001).
38. M.O. Distler, H. Merkel, M. Weis, *Proceedings of the 12th IEEE Real Time Congress on Nuclear and Plasma Sciences, Valencia (2001)*, IEEE Trans. Nucl. Sci., Vol. **49**, No. 2, Part 1a.2 (2002).
39. K. Bätzner *et al.*, Nucl. Phys. B **76**, 1 (1974).
40. J.J. Kelly *et al.*, Phys. Rev. Lett. **95**, 102001 (2005).
41. J.J. Kelly *et al.*, nucl-ex/0509004.
42. P. Senger, Nucl. Instrum. Methods A **327**, 393 (1993).